The limitations of Lindhard ~~theory~~ to predict the ~~ionization~~ produced by nuclear recoils at the lowest energies

model

"energy given to electrons"
= ionization + scintillation in e.g. liquid nobles

see also

Phys. Rev. D **91** 083509 (2015)

Caveats

- This is mostly a theory talk
- No theorist can exactly solve this problem (collective many-body scattering)
- I'm no theorist

Motivation

- Measuring low-energy nuclear recoils signals is clearly tough (hence this workshop)
- I've worked on it experimentally in both xenon and argon
- Models can be helpful, even if only to offer guidance
- I wanted a better understanding of the uncertainties and limitations of the Lindhard model

An experimentalist descends from an ivory tower, having encountered the Lindhard model

Exodus 34:29

The big picture tends to gloss over the atomic physics

pictures tend to influence our thinking

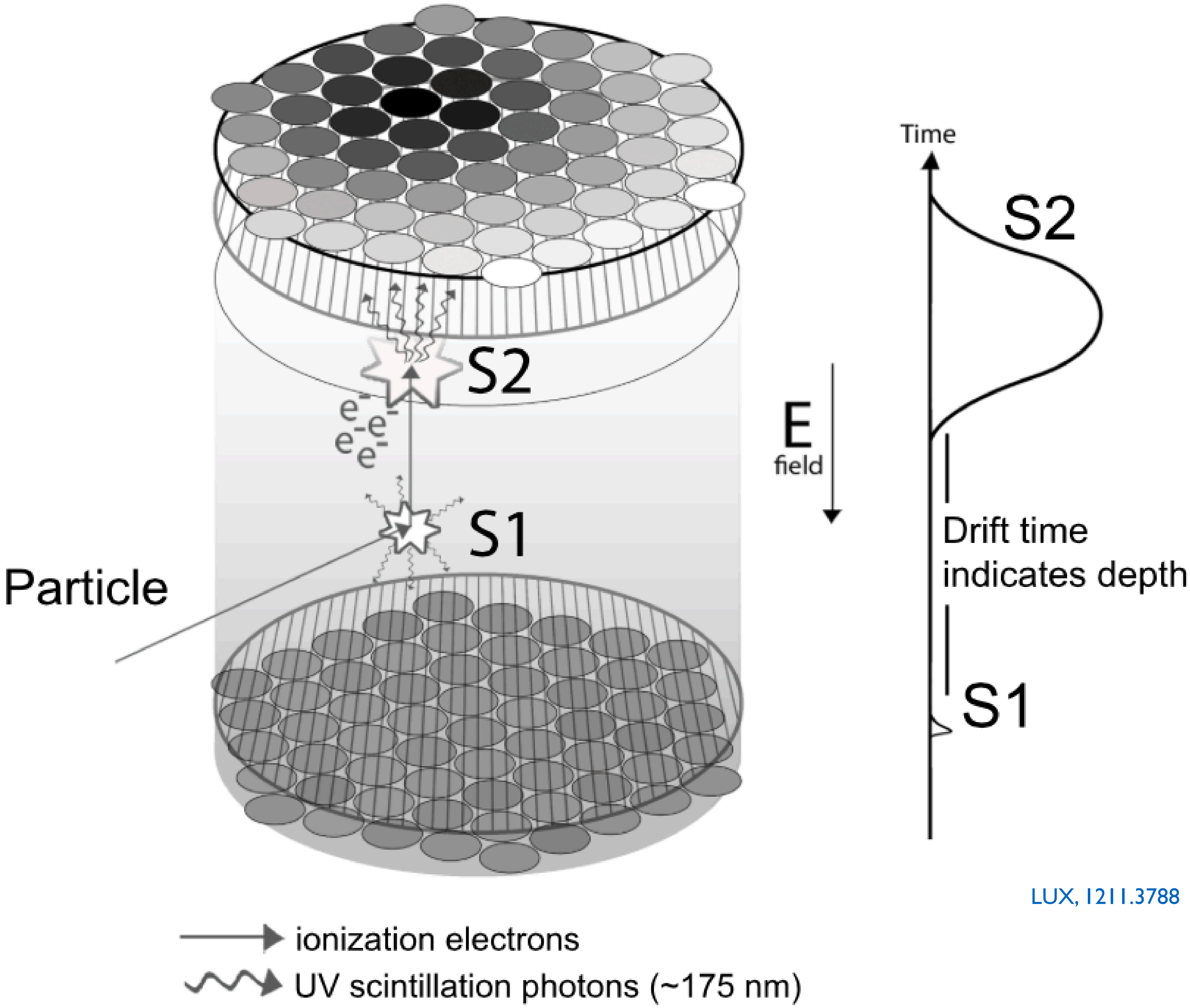

LUX, 1211.3788

Example from 2010: drawn-out debates over where to draw the line

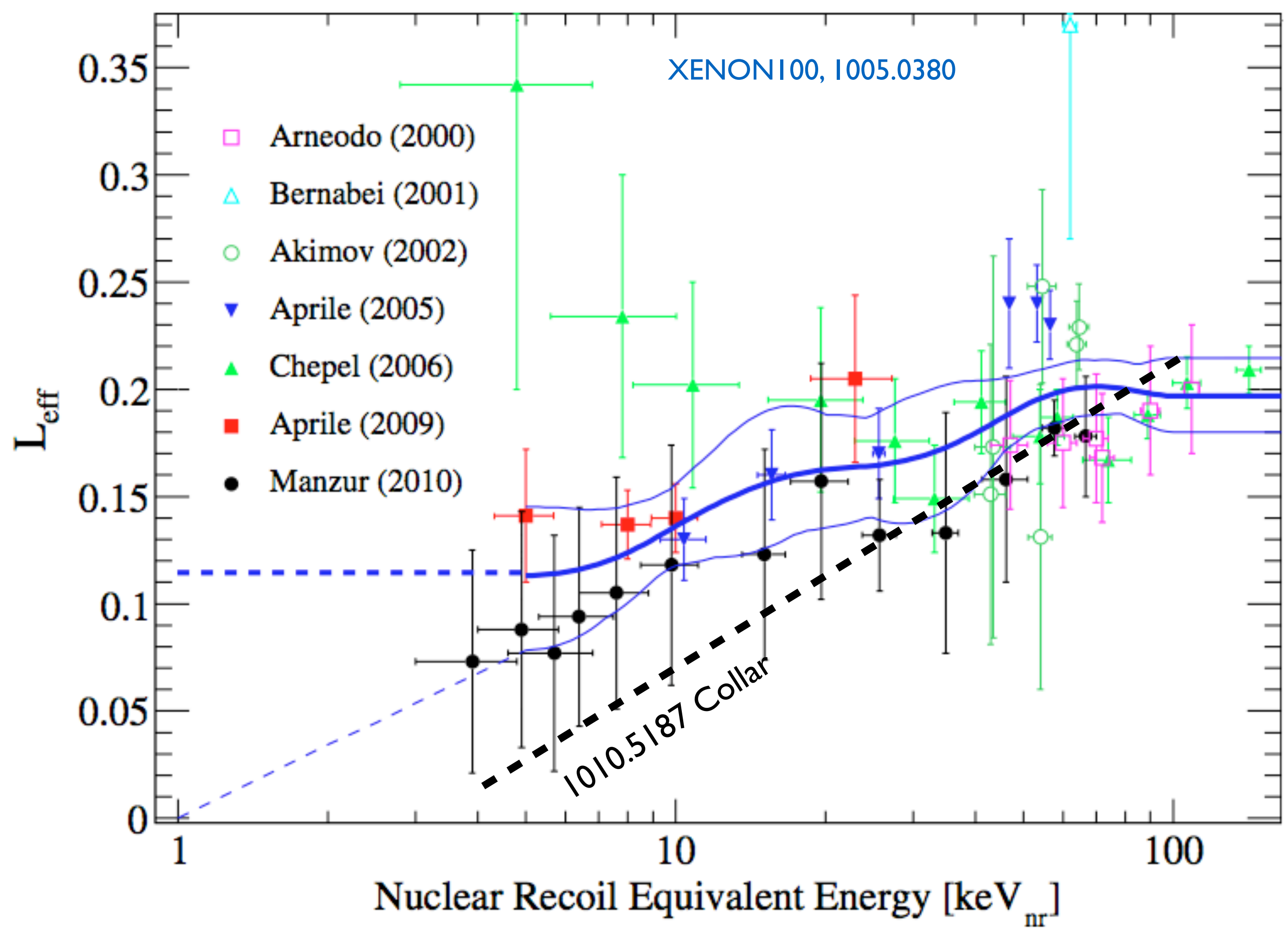

- Since 2010, understanding of xenon nuclear recoil signal yields has grown, cf. Dahl thesis (2009), 1101.6080 (PS & Dahl), 1106.1613 (NEST)

- My take aways from the arxiv arguments of 2010:
  - a physical model for signal quenching is important (if only as a guide)
  - ***two questions are without answers:***
    - *1- is there a kinematic cutoff in signal production?* -YES
    - *2- shouldn't the Lindhard model apply to all homogenous targets?* -YES

First question: is there a kinematic cutoff?

quoting from 1005.0838

right idea, wrong physical picture

> The marked drop in $\mathcal{L}_{\rm eff}$ at low energies in the experiments that the XENON100 collaboration has ignored may be understood from simple two-body kinematics affecting the energy transfer from a xenon recoil to an atomic electron. As already discussed within the context of the MACRO experiment [10], a kinematic cutoff to the production of scintillation is expected whenever the minimum excitation energy E_g of the system exceeds

[10] Phys. Rev. D 36 311 (1987)

$$E_{\rm max} = 2m_e v(v + v_e)$$

$$V_{cutoff} \approx E_g / 2m_e v_F$$

the formulae, applied to nucleus-electron scattering, result in calculated cutoff recoil energies of ~39 keV in Xe and ~0.1 keV in Ge. This is not the right thing to do.

NB: as $E_R \rightarrow 0$, atoms are basically standing still, but electrons have $v \sim \alpha$

Second question: wouldn't the Lindhard model apply to all (homogenous) targets?

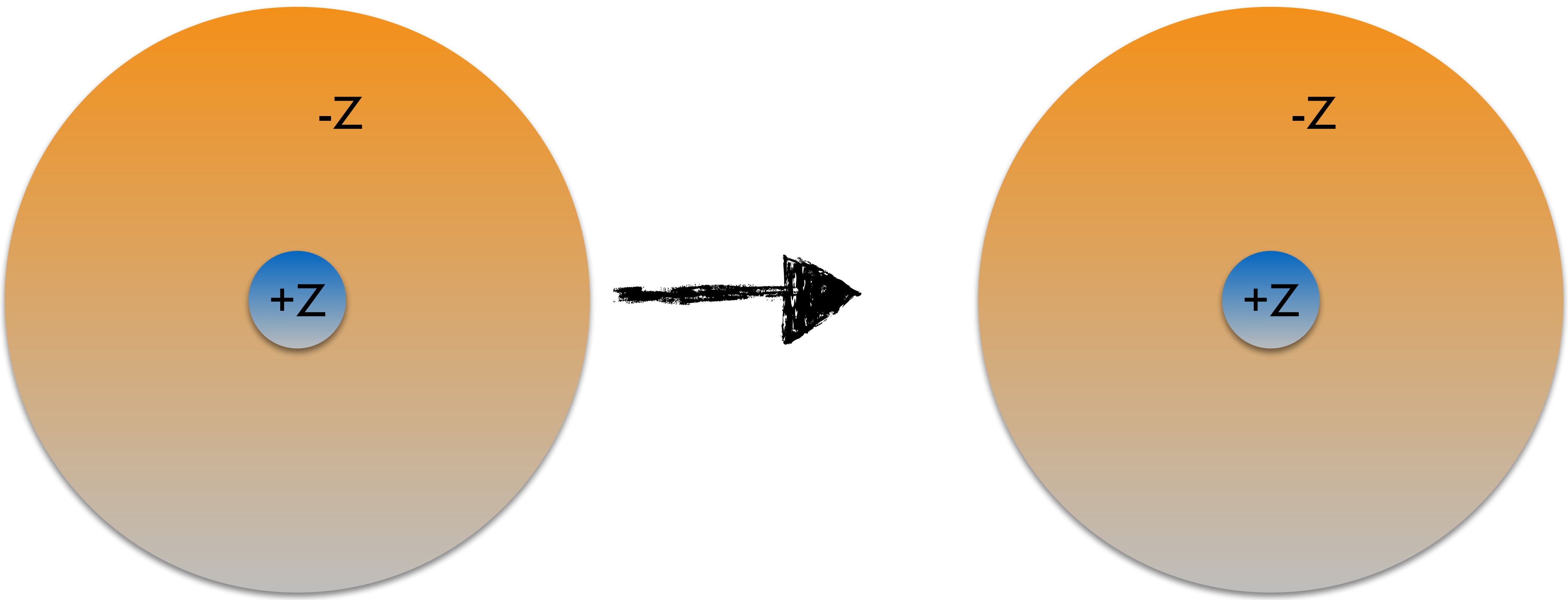

- two body screened Coulomb nuclear scattering
- average electronic scattering (stopping, really: projectile atom perturbs free electron gas)

Simplify the problem to effective two-body kinematics

The origin of signal:

- nucleus gets a kick (from a neutron, a neutrino, dark matter)
- atom recoils
- creates secondary recoils
- cascade continues until atoms are thermalized
- each collision might excite or ionize a target or projectile atom
- but, individual electron collisions?? too complicated. average over electronic energy losses

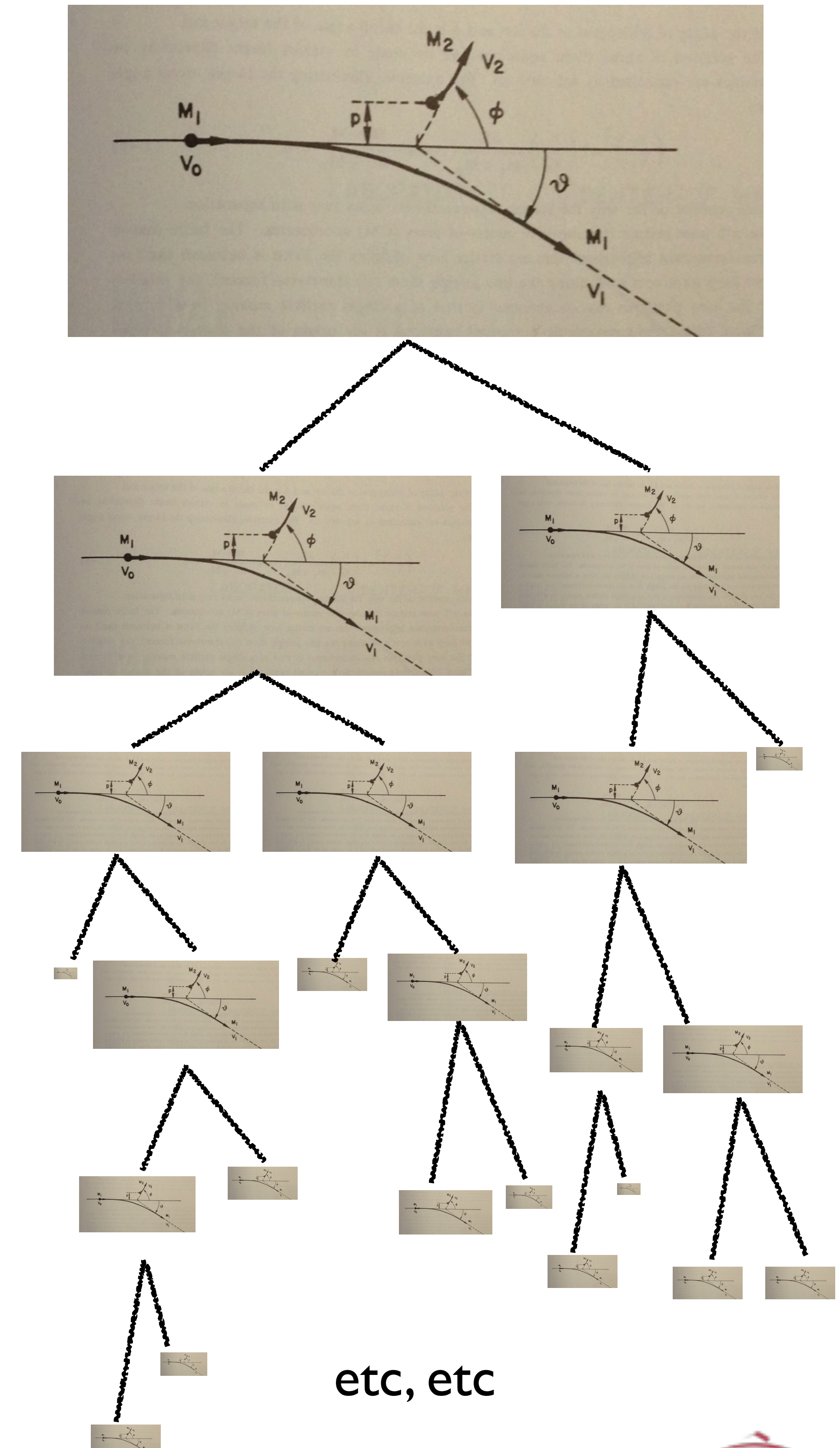

The Lindhard model, single slide version

reduced energy

nuclear energy loss

$$k\varepsilon^{1/2}\bar{\nu}'(\varepsilon) = \int_0^{\varepsilon^2} \frac{dt}{2t^{3/2}} f(t^{1/2})$$

$$\times \left\{ \bar{\nu}\left(\varepsilon - \frac{t}{\varepsilon}\right) - \bar{\nu}(\varepsilon) + \bar{\nu}\left(\frac{t}{\varepsilon}\right) \right\}$$

electronic energy loss

target atom after collision

projectile atom before collision

projectile atom after collision

- Integrate over the cascade, obtain a solution for $\bar{\nu}$ (the energy given to atomic motion)
- A parameterization of the solution is

$$\bar{\nu}(\varepsilon) = \frac{\varepsilon}{1 + kg(\varepsilon)} \quad \text{which leads directly to} \quad f_n \equiv \frac{\varepsilon - \bar{\nu}}{\varepsilon} = \frac{kg(\varepsilon)}{1 + kg(\varepsilon)}$$

f_n is what we usually call the quenching factor

The model works pretty well!

$$E_{\rm nr} = \epsilon(n_\gamma + n_e)/f_n$$

$$E_{\rm nr} = \epsilon(\cancel{n_\gamma +}\, n_e)/f_n$$

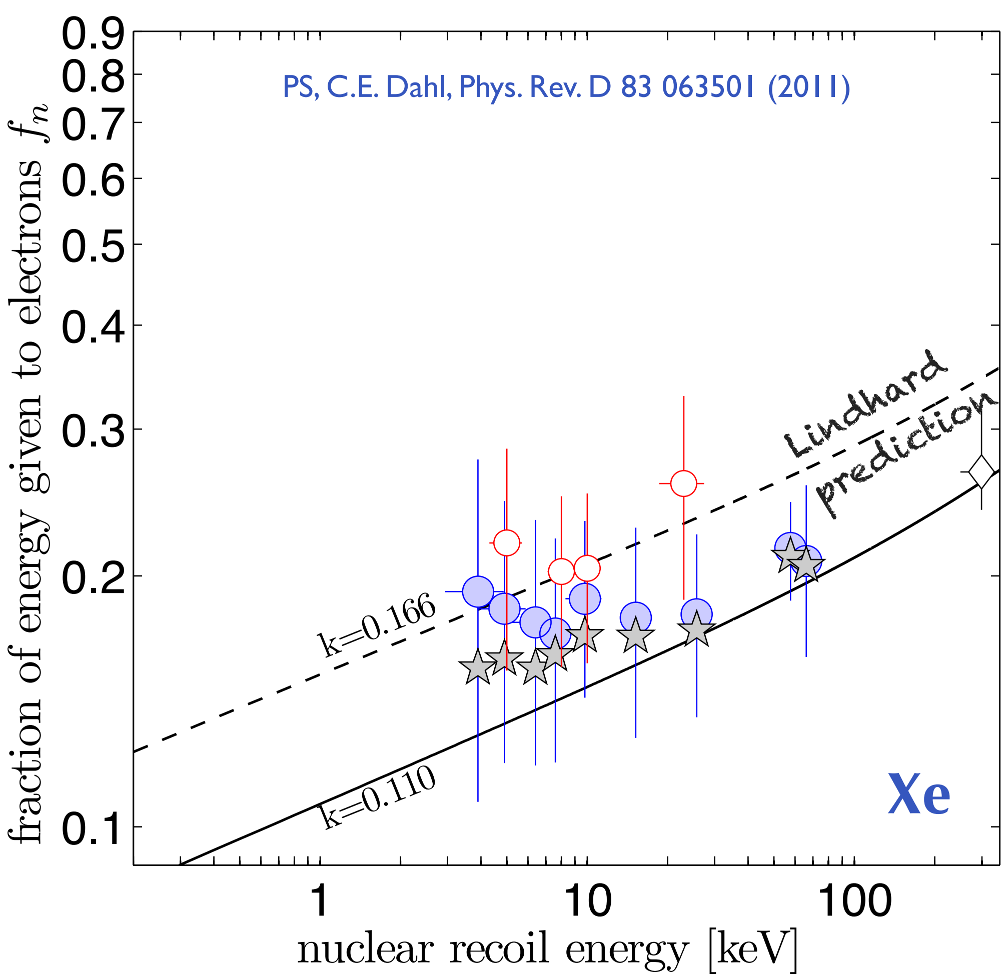

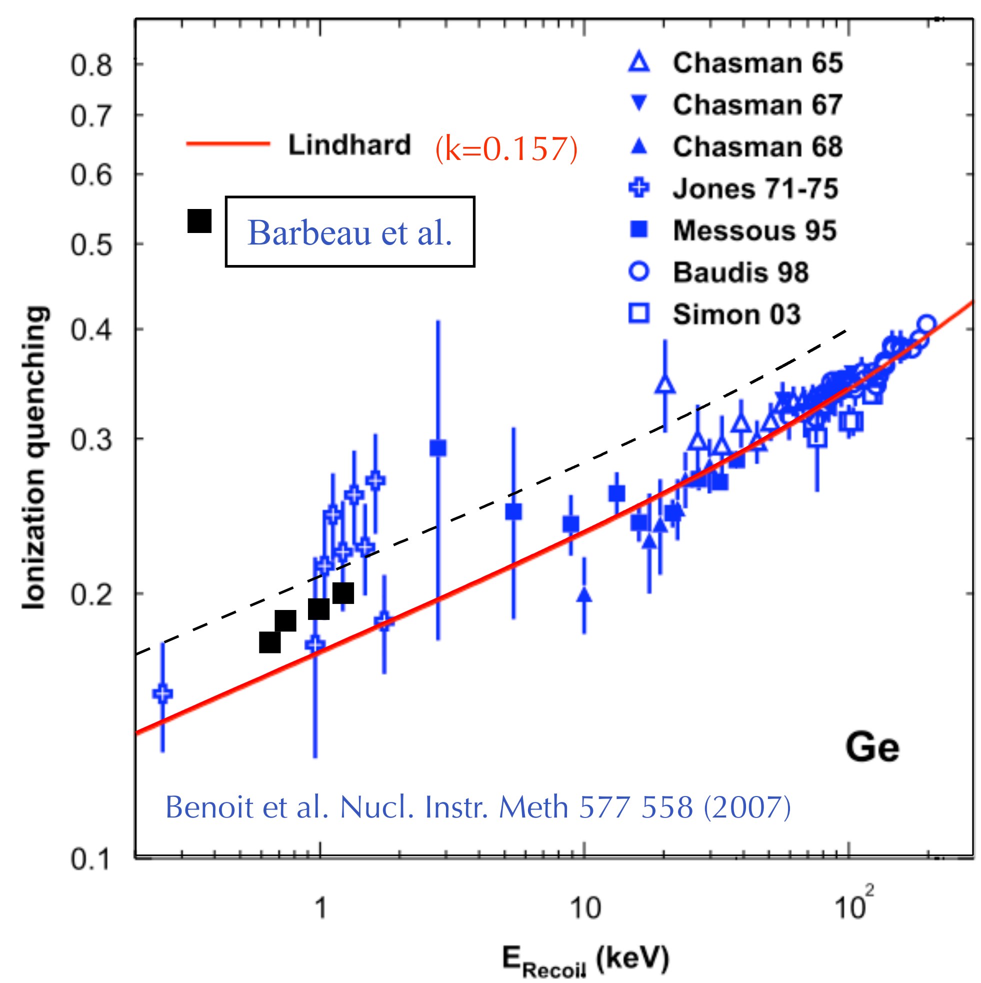

NB: new measurements from LUX extend down to ~1 keV. See J Verbus talk from yesterday.

The model works pretty well!

$$E_{\mathrm{nr}} = \epsilon(n_\gamma + n_e)/f_n$$

$$E_{\mathrm{nr}} = \epsilon(\cancel{n_\gamma +} n_e)/f_n$$

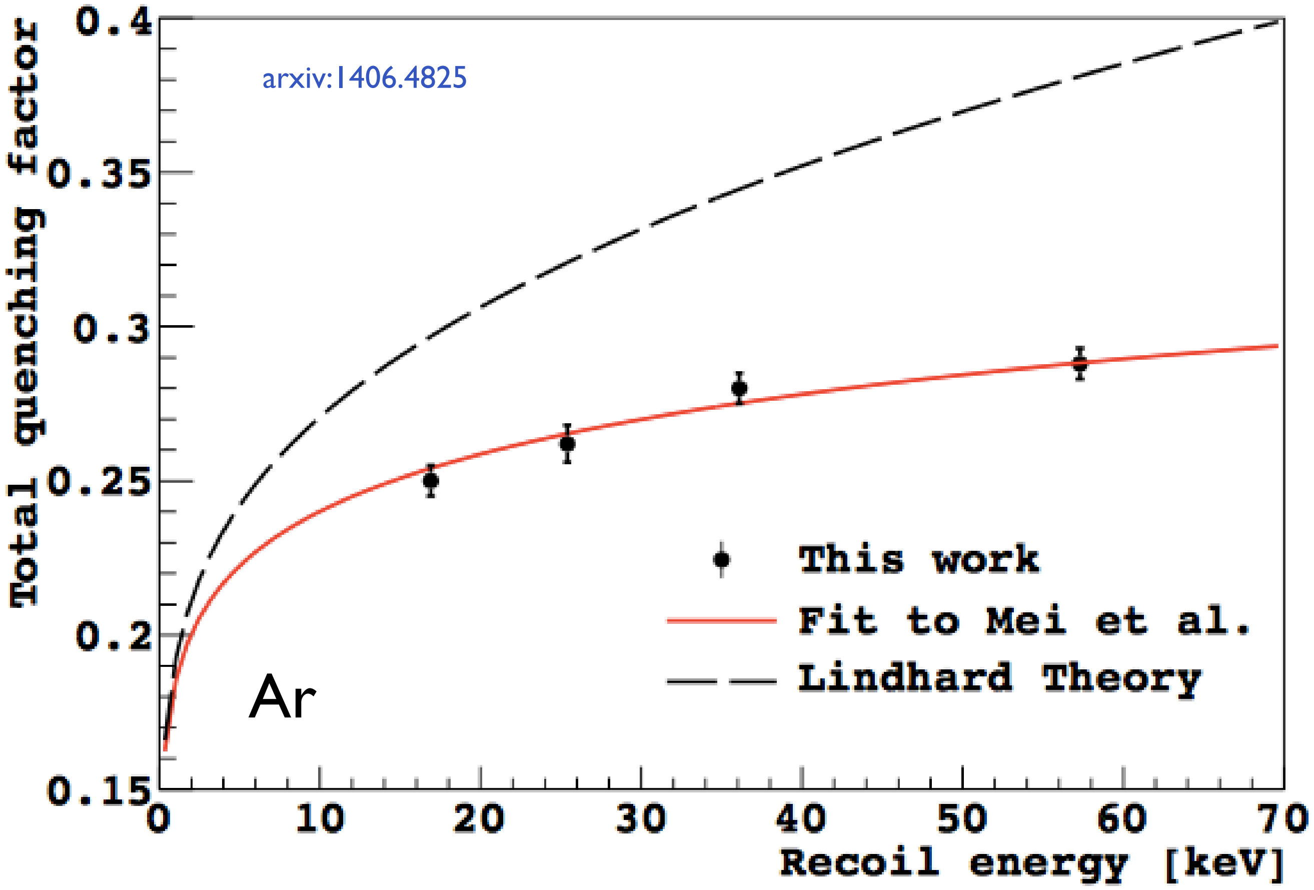

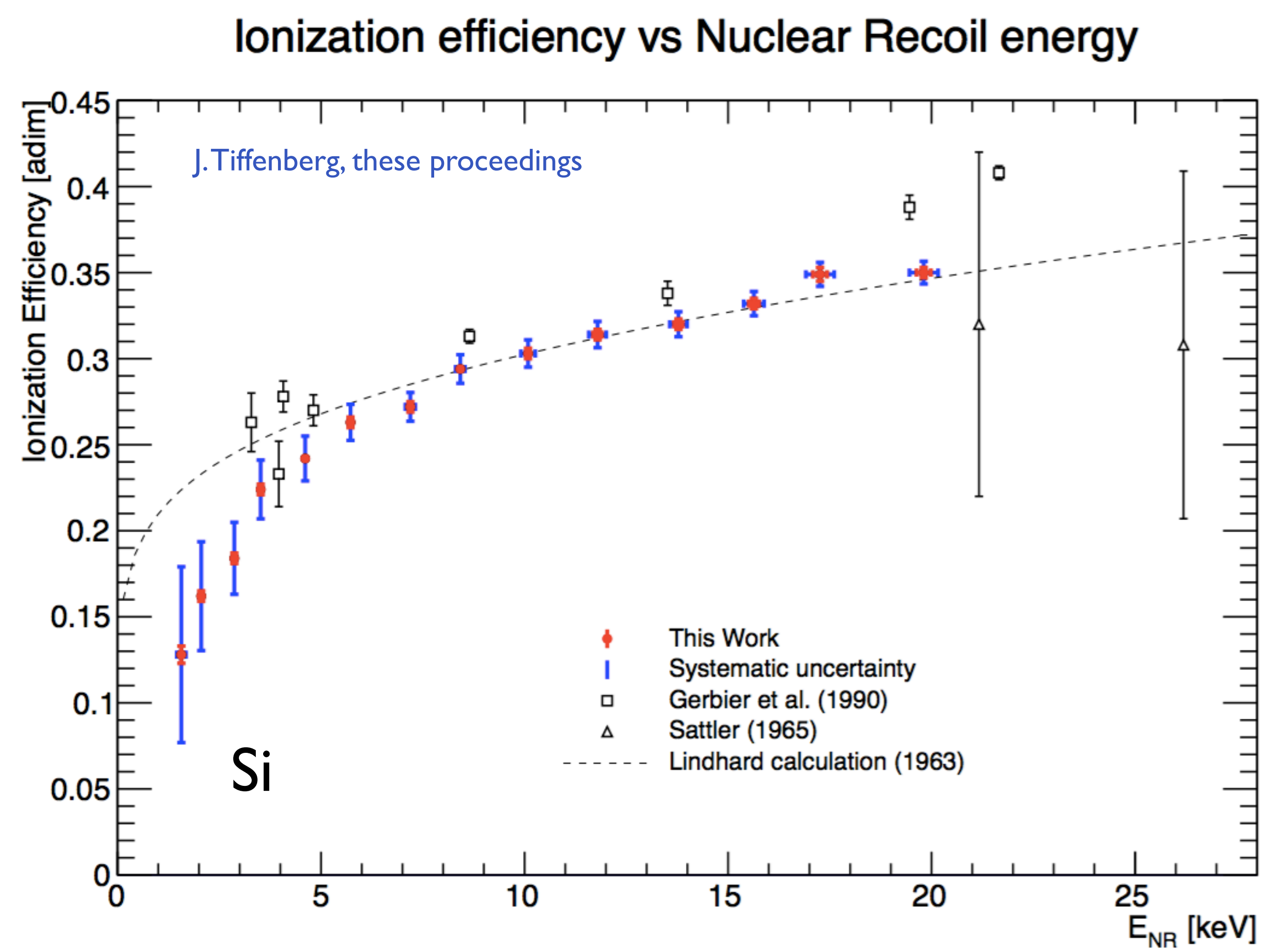

Approximations in nuclear scattering treatment

Ziegler, Biersack, Littmark, "The stopping and range of ions in solids" (1985)

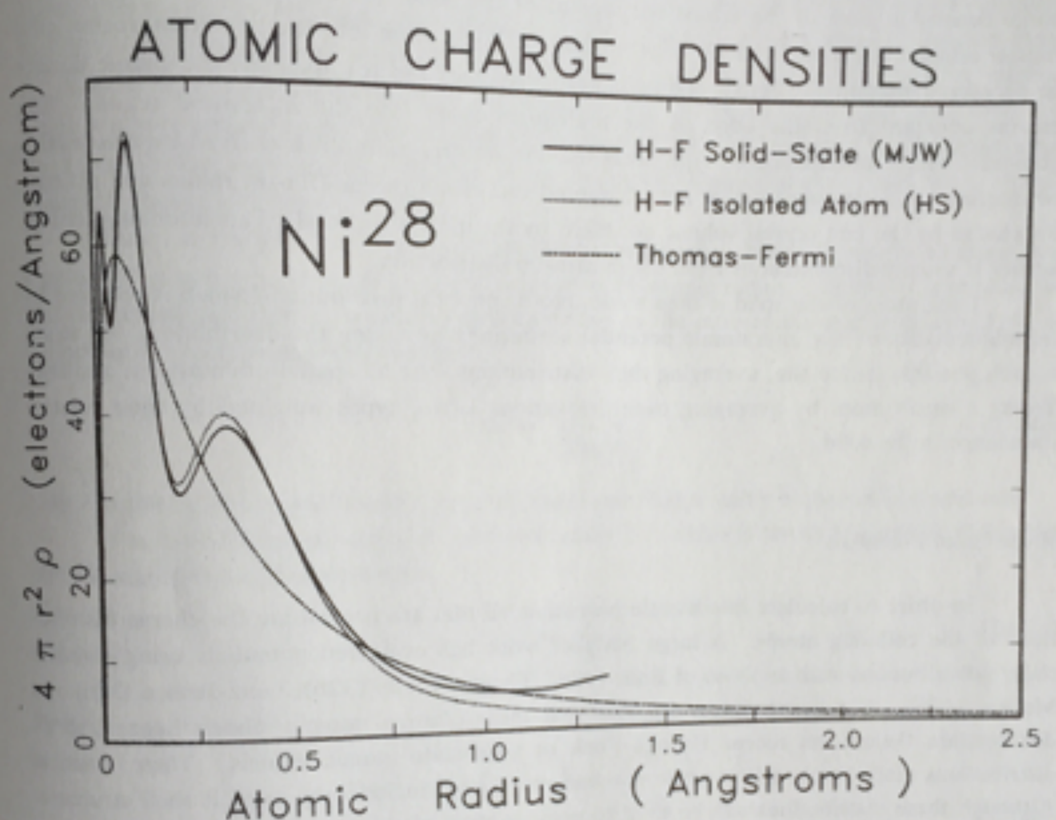

Figure (2-5) The charge distributions of nickel atoms. The ordinate is plotted in units of $4\pi r^2\rho$, where ρ is the electronic density, so that the shell structure is clearly seen, and also so the area under the curve equals 28, the atomic number of nickel. The smooth dashed curve is the Thomas-Fermi distribution and it shows no shell structure. The dotted curve is a Hartree-Fock atom calculated by Herman-Skillman (HS) for isolated atoms (see ref. 63d). The solid line is for a Hartree-Fock nickel atom in its normal face-centered cubic structure. The structure is similar to the HS atom for the inner electronic structure, but is quite different for the binding and conduction electrons. The atom shown is the spherical average over all nickel substitutional atoms in the crystal. The difference in outer shell electronic structure is very important for low energy electronic stopping where it may change the stopping power by a factor of two for ions of velocity 25 keV/amu.

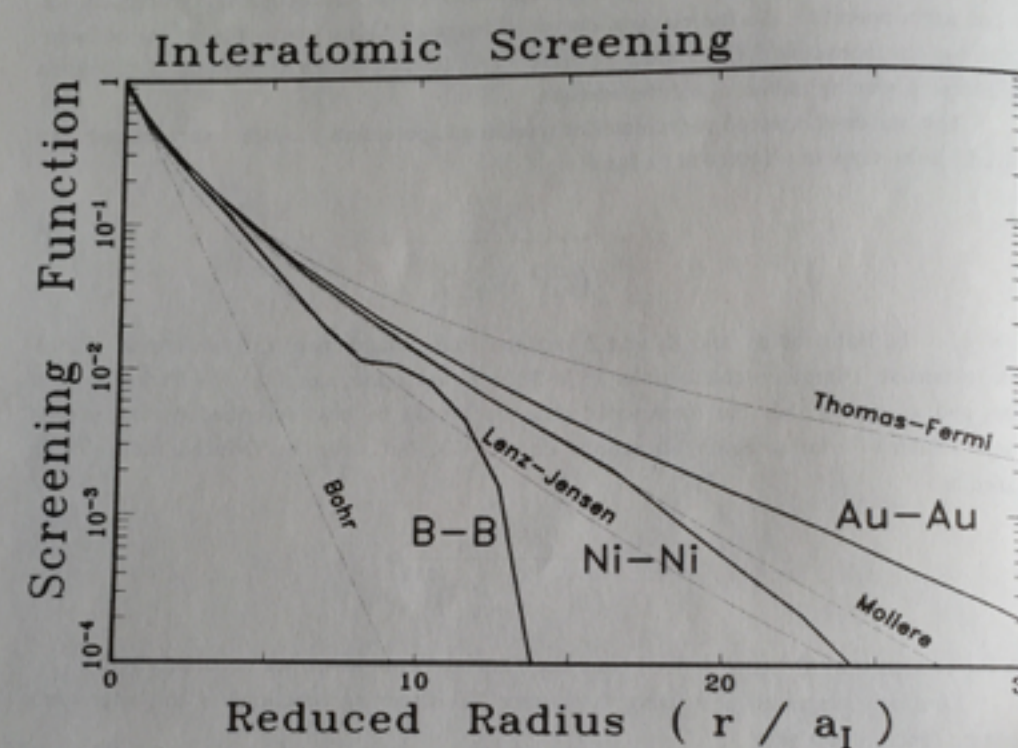

interatomic screening length

$a_I = 0.8853\, a_0 / (Z^{-1/3}\sqrt{2})$

$a_I \sim 0.1$

differs from single atom screening length by factor $1/\sqrt{2}$

Figure (2-8) The interatomic screening functions for atom-atom combinations of B-B, Ni-Ni and Au-Au. These identical pairs were selected so they could be compared with the screening functions of single atoms in figure (2-8). These screening functions were calculated with equation (2-31) using the solid-state charge distributions tabulated in the Appendix. The classical single-atom screening functions are shown. These may be extended to interatomic screening functions by redefining the screening parameter, a, from the single-atom definition of a_{TF} in equation (2-46), to an interatomic definition of a_I as argued for equations (2-53) to (2-55). The plot shows that the Moliere screening function is accurate to about a factor of 2 or 3 to detailed solid-state calculations.

Approximations in electron scattering ("electronic stopping") treatment

$$S_e = (8\pi e^2 a_0 \xi Z_1 Z_2 / Z)(v/v_0), \quad = k\varepsilon^{1/2} \tag{1}$$

where $\xi = Z_1^{1/6}$, $Z = (Z_1^{2/3} + Z_2^{2/3})^{3/2}$, and $a_0 = \hbar^2/me^2$.

- $d\varepsilon/d\rho = k\varepsilon^{1/2}$
- all calculations predict this basic behavior

Markin et al, Phys. Rev. Lett 103 113201 (2009)

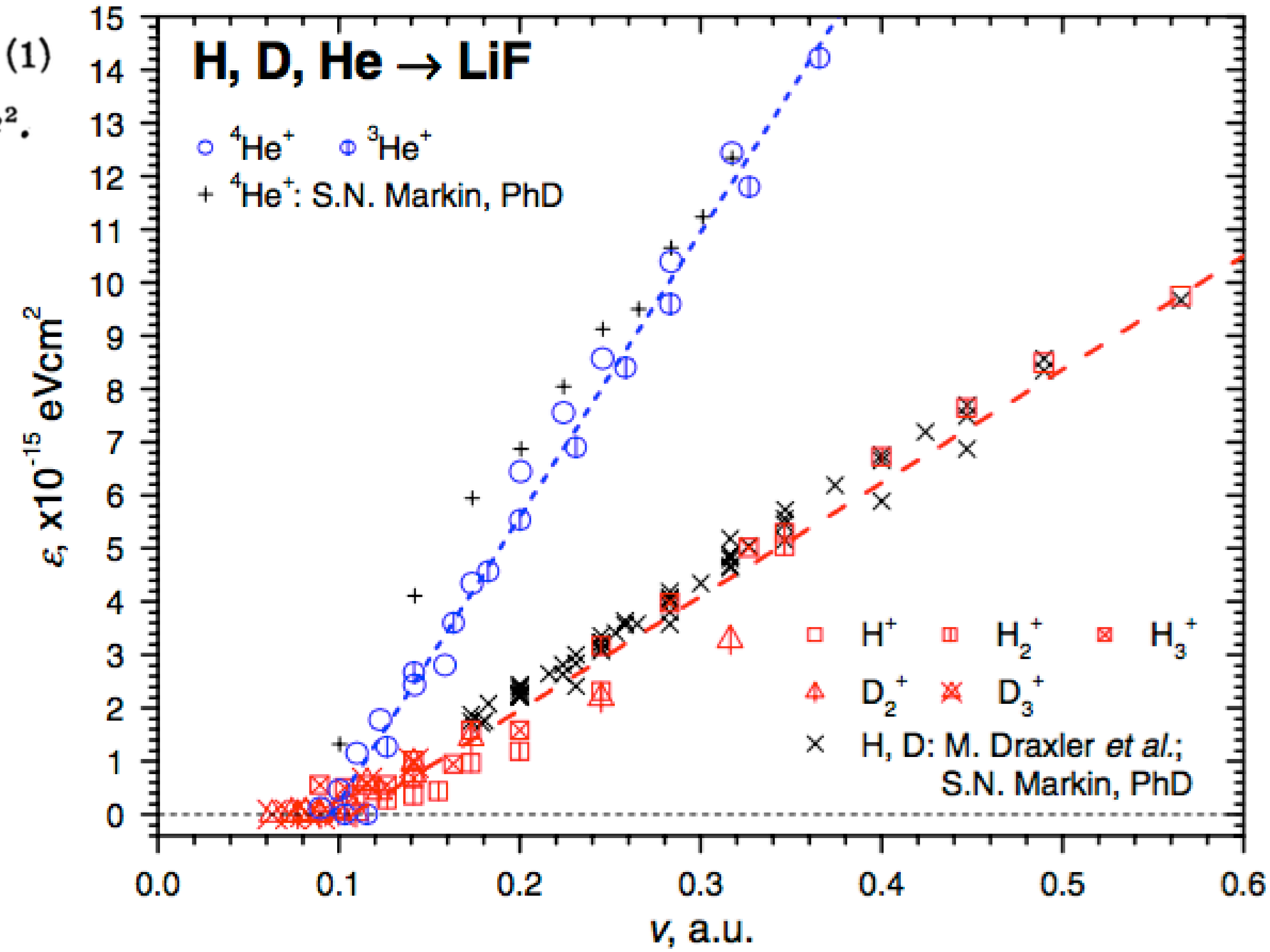

FIG. 2 (color online). Electronic stopping cross section ε of H, D, and He ions in LiF as a function of the projectile velocity v. Also shown are the data for H ions from [13] and for He ions from [24].

Approximations in electron scattering (“electronic stopping”) treatment (II)

- calculations supported by data, but
  - problem #0: not a lot of data
  - problem #1: a non-zero x intercept is often observed
  - problem #2: semiconductors are expected to show deviation from velocity-proportional stopping at low energies, due to band gap
- should think of liquid nobles as large band gap insulators in this context

Markin et al, Phys. Rev. Lett 103 113201 (2009)

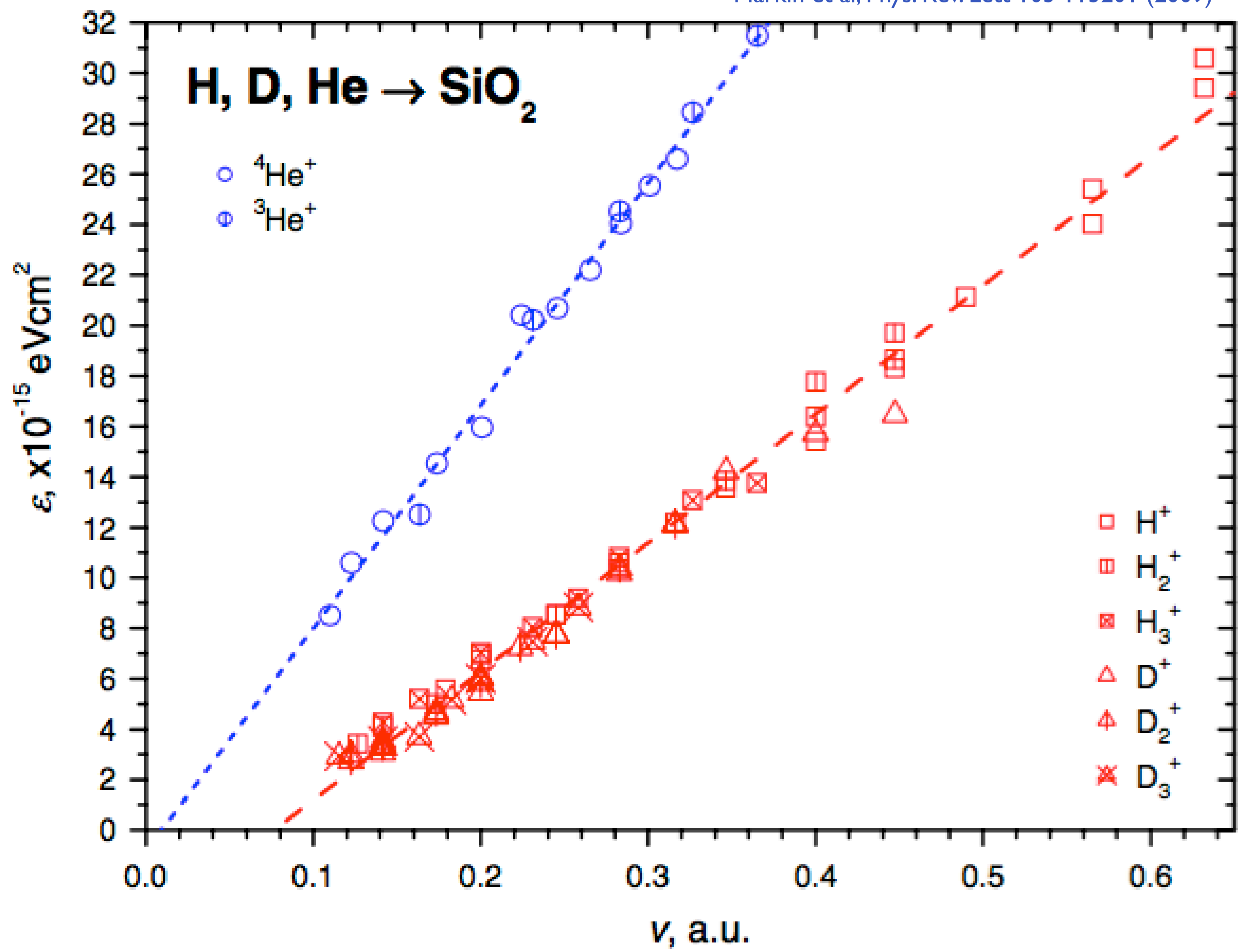

FIG. 4 (color online). Electronic stopping cross section ε of H, D, and He ions in SiO_2 as a function of projectile velocity v.

Variations in electron scattering ("electronic stopping") calculations

- Large uncertainty in k is possible
- Ge happens to be at a sweet spot (all calculations converge)
- Si appears to be approximately sweet
- Liquid nobles may differ (drastically) from naive Lindhard k

Land et al, Phys. Rev. A 16 492 (1977)

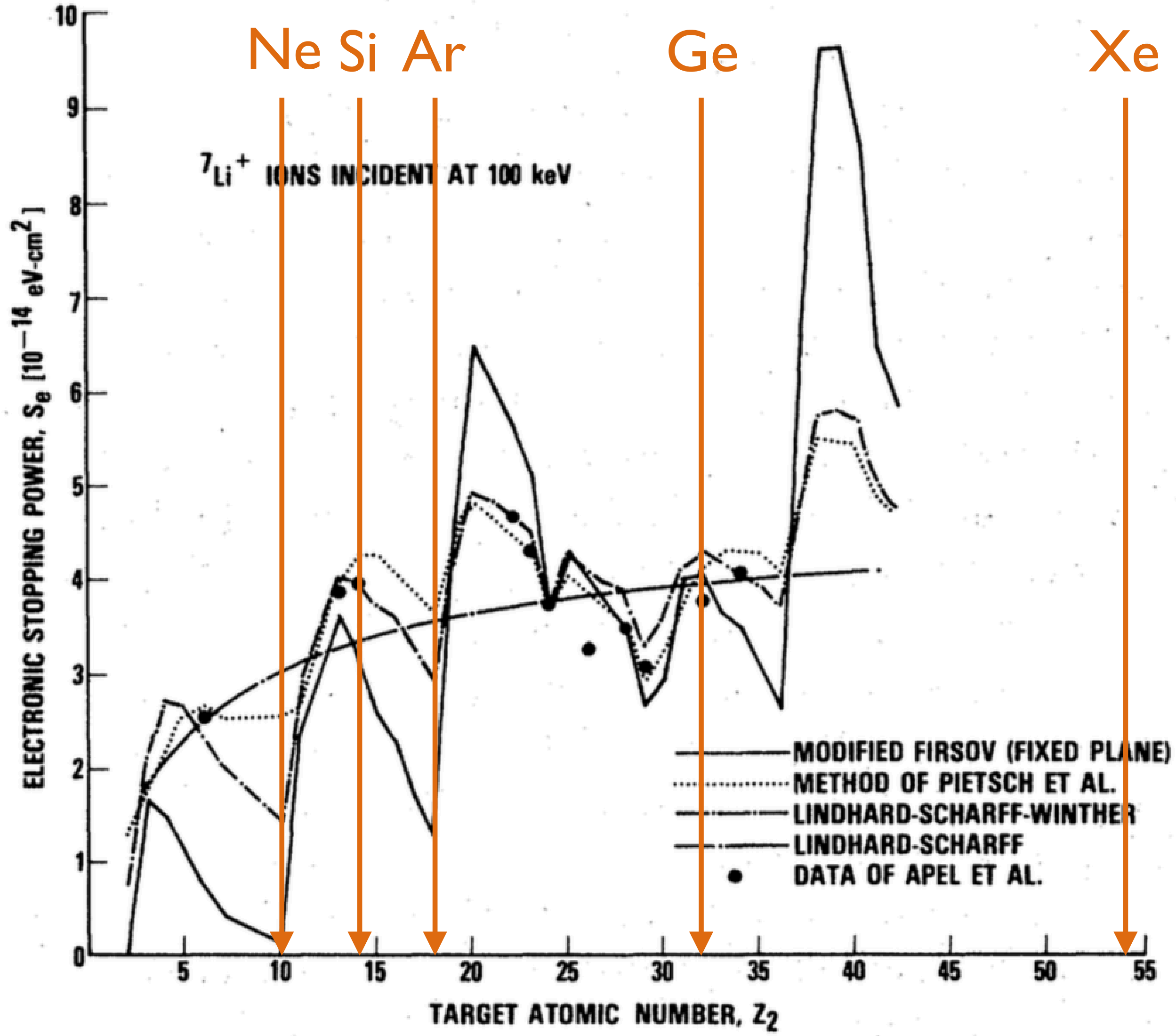

FIG. 4. Comparison of theoretical results for the electronic stopping power of 100-keV ^{7}Li$^+$ ions based upon the modified Firsov method, Lindhard-Scharff-Winther method, and the method of Pietsch *et al.* Experimental data are included.

Conclusions thus far…

The Lindhard model…

- Makes numerous approximations in order to distill solid state atomic scattering into a tractable problem
  - results in quantitative predictions that appear to agree fairly well for a number of targets
  - it is difficult to accurately quantify the uncertainties, but a range can be inferred
- Low velocity behavior of electronic stopping is expected to decrease in materials with a band gap
  - difficult to quantify
  - may not be a significant effect (?)
- Does not account for atomic binding
  - intuitively this must make a difference at low energy
  - can be re-instated in model…

First simple tweak to the model: improve the parameterization

- add a constant energy term q and re-solve the integral equation (slide 9)
- result is dashed orange curve

$$\bar{\nu}(\varepsilon) = \frac{\varepsilon}{1 + kg(\varepsilon)} + q \quad \rightarrow \quad f_n = \frac{kg(\varepsilon)}{1 + kg(\varepsilon)} - q/\varepsilon$$

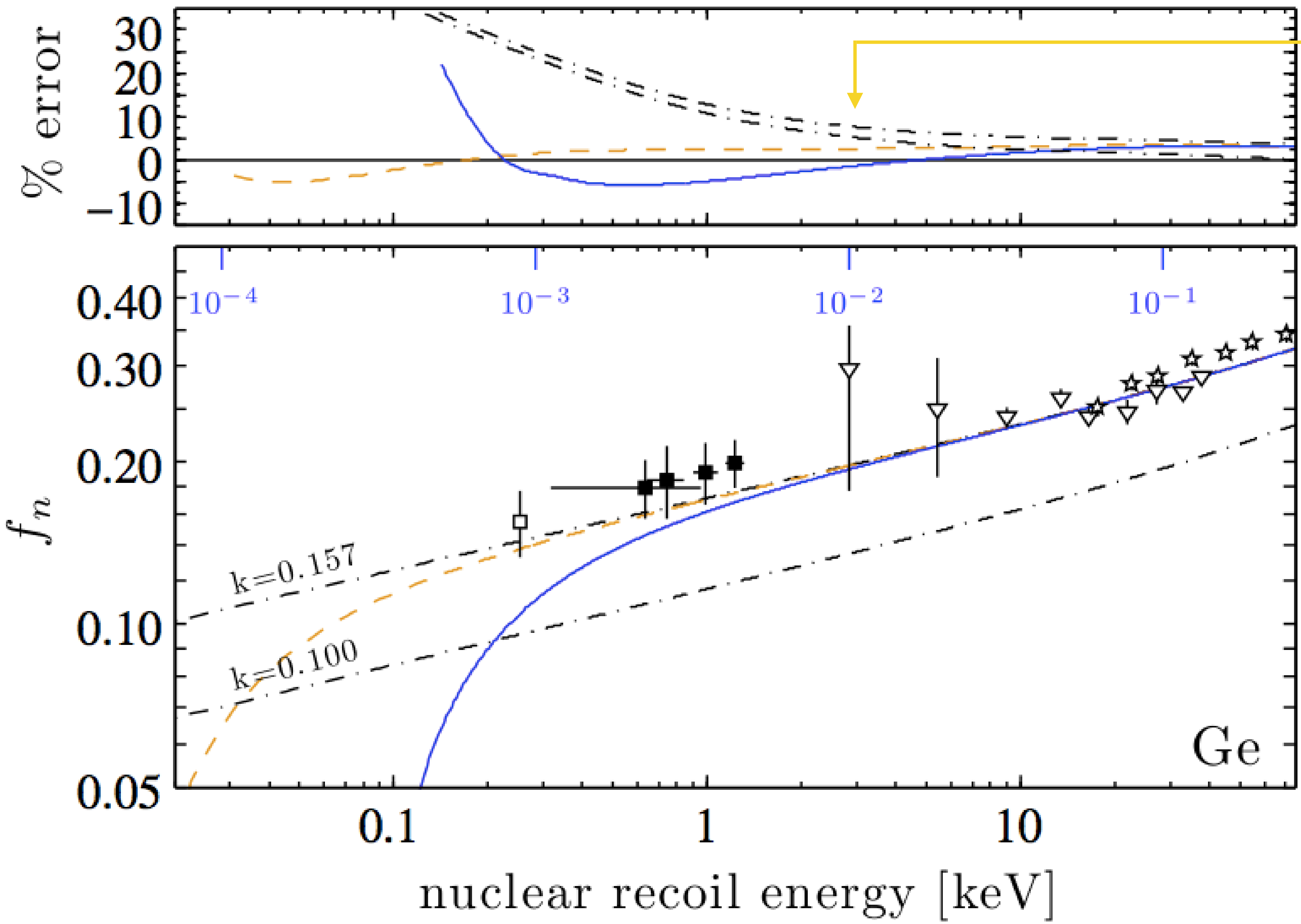

Second simple tweak to the model: account for electron binding energy

- replace the term $\bar{\nu}(t/\varepsilon)$ with $\bar{\nu}(t/\varepsilon - u)$ and re-solve the integral equation (slide 9)
- u is the average energy required to ionize an electron (the w-value)
- result is solid blue curve

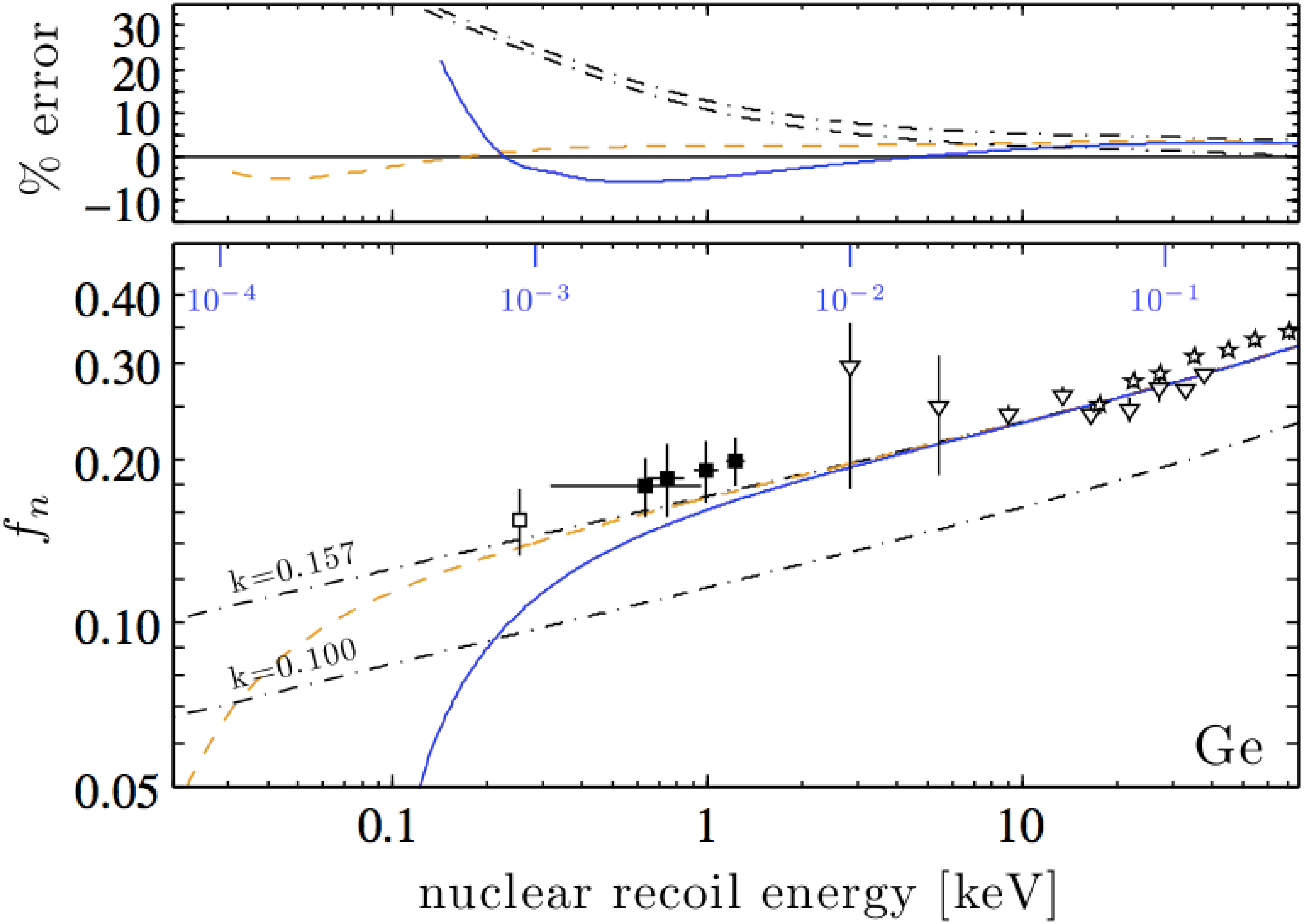

Result for Si

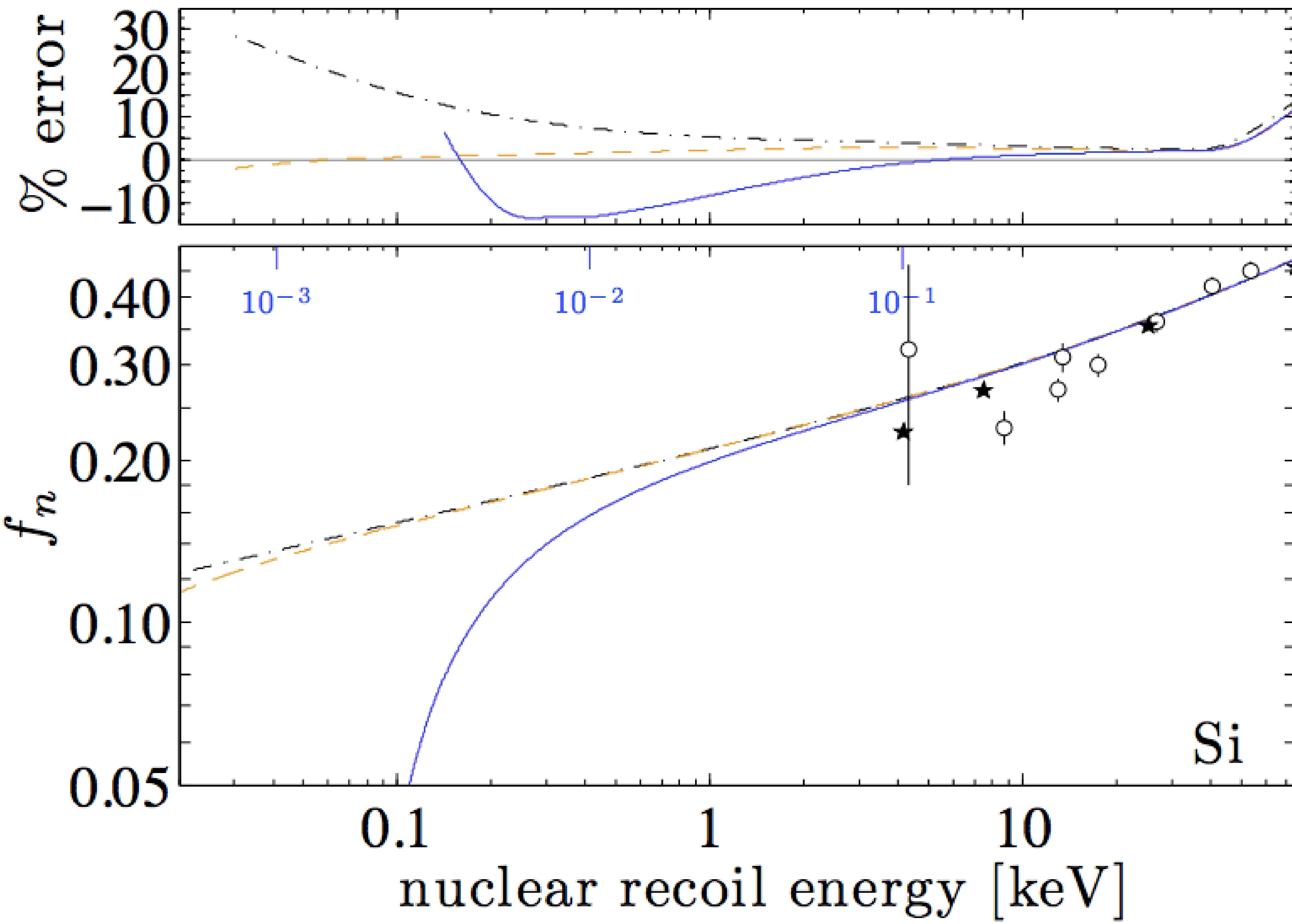

Result for Xe

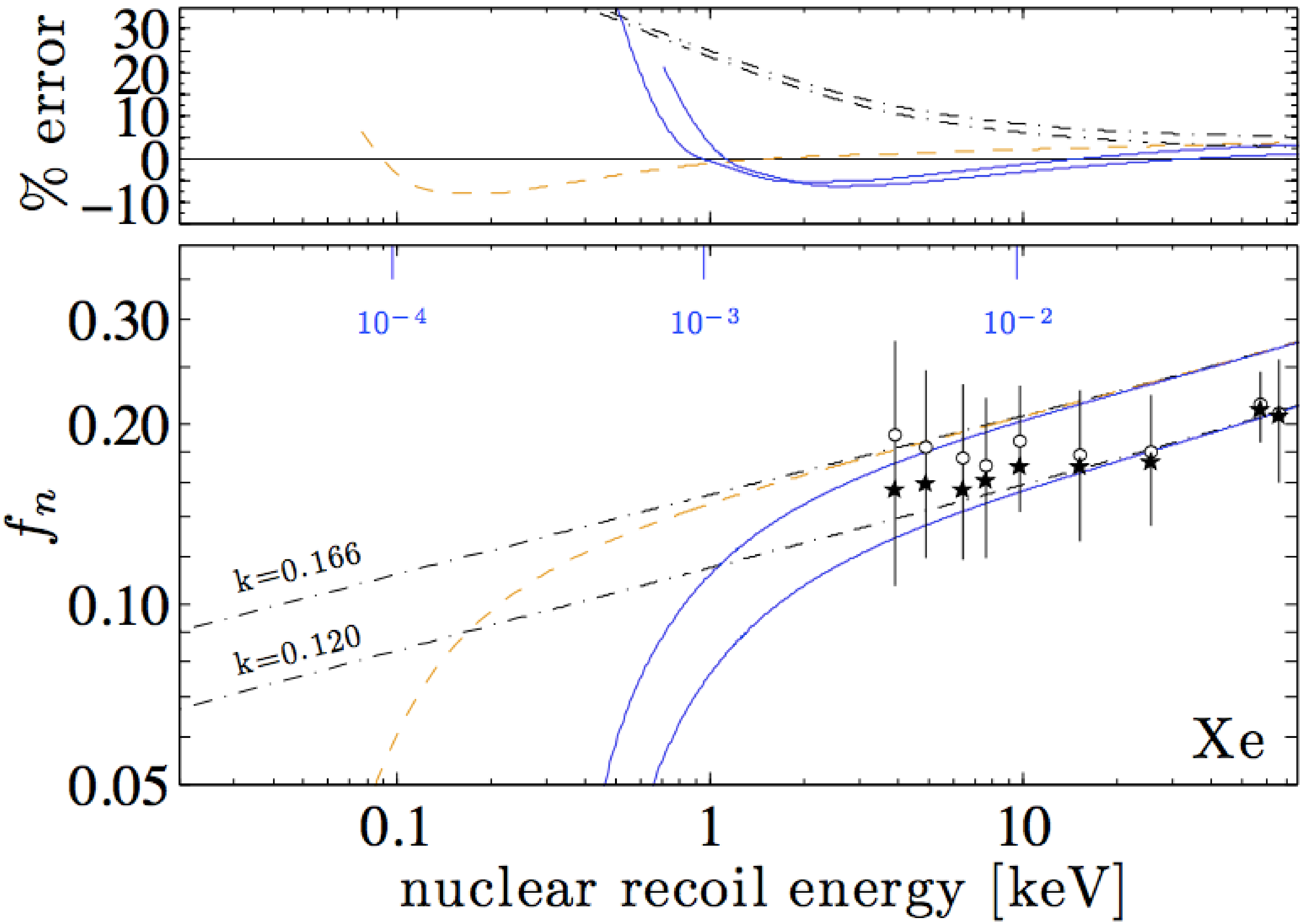

Result for Ar

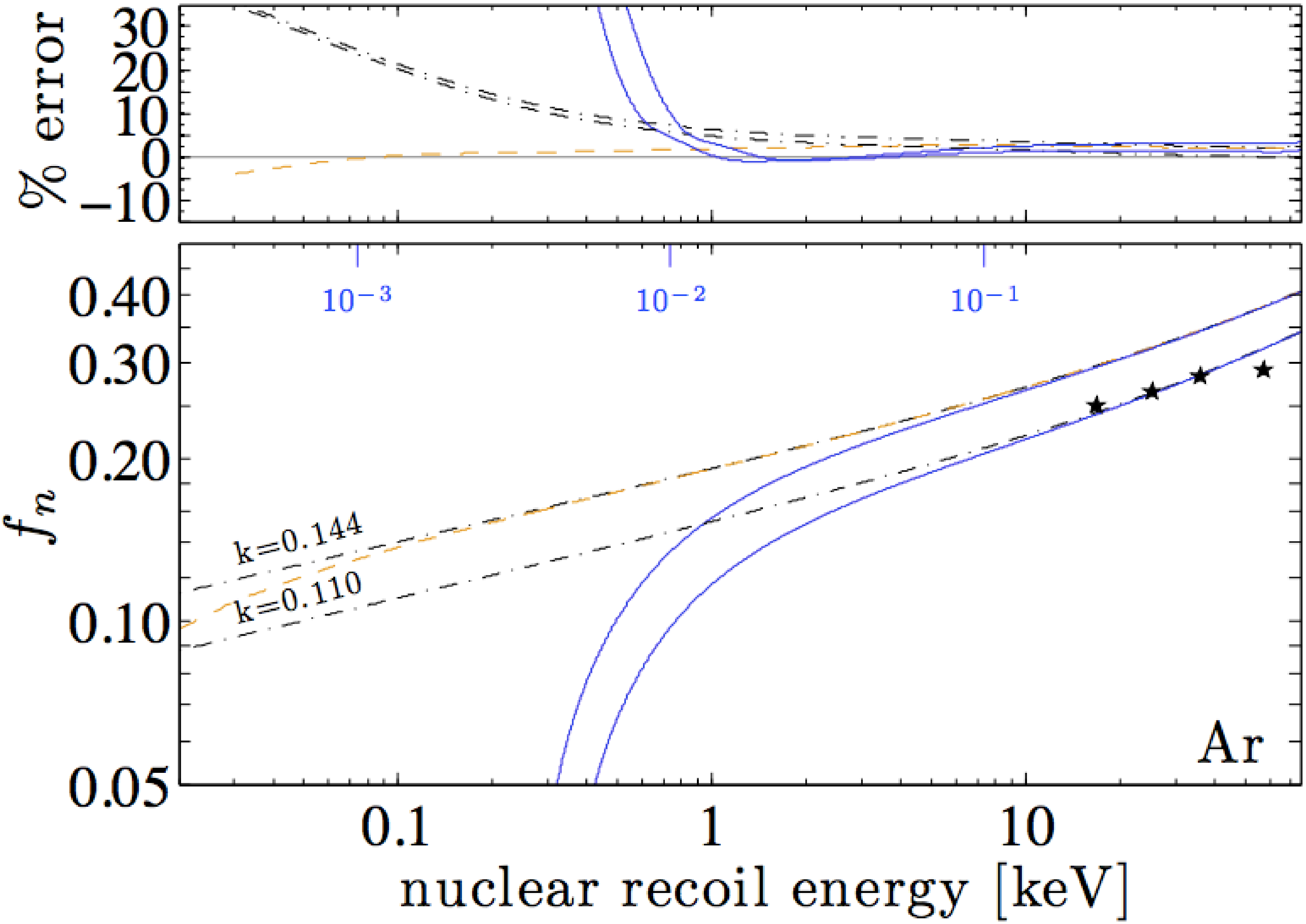

This matters if you are…

•Searching for O(1) GeV dark matter via nuclear recoil scattering
•Searching for CENNS from low-energy (e.g. reactor) neutrinos

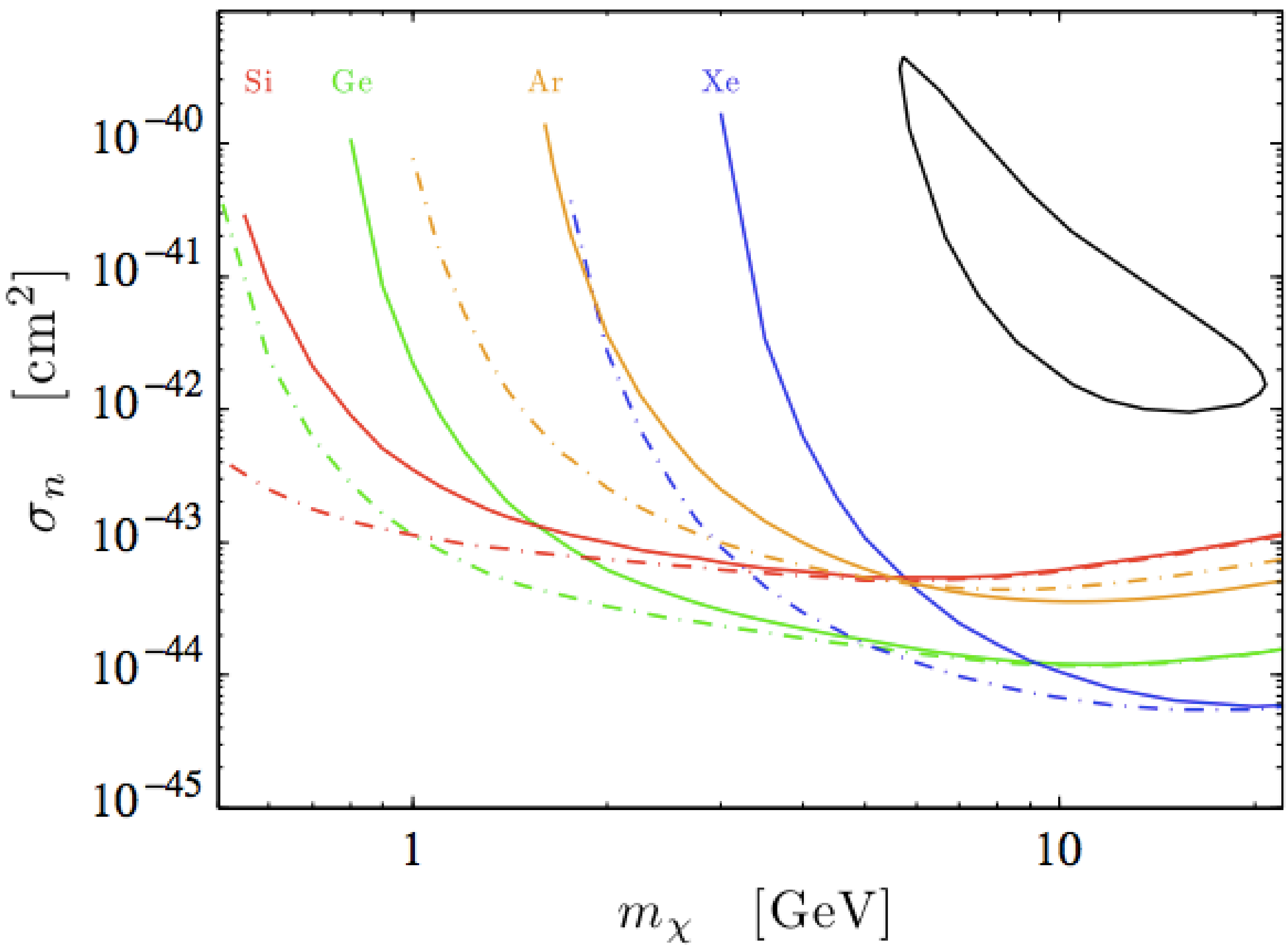

Summary

- cf. slide 18
- Kinematic cutoff is a generic prediction of Lindhard model
  - quantitative prediction, but
  - significant uncertainties in low-energy predictions of the model
- Low-energy extrapolations of Lindhard model should probably treat the basic prediction as an upper bound (cf. problem #1 and #2 on slide 16)
- Experimental data are essential

34

Ziegler, Biersack, Littmark, "The stopping and range of ions in solids" (1985)

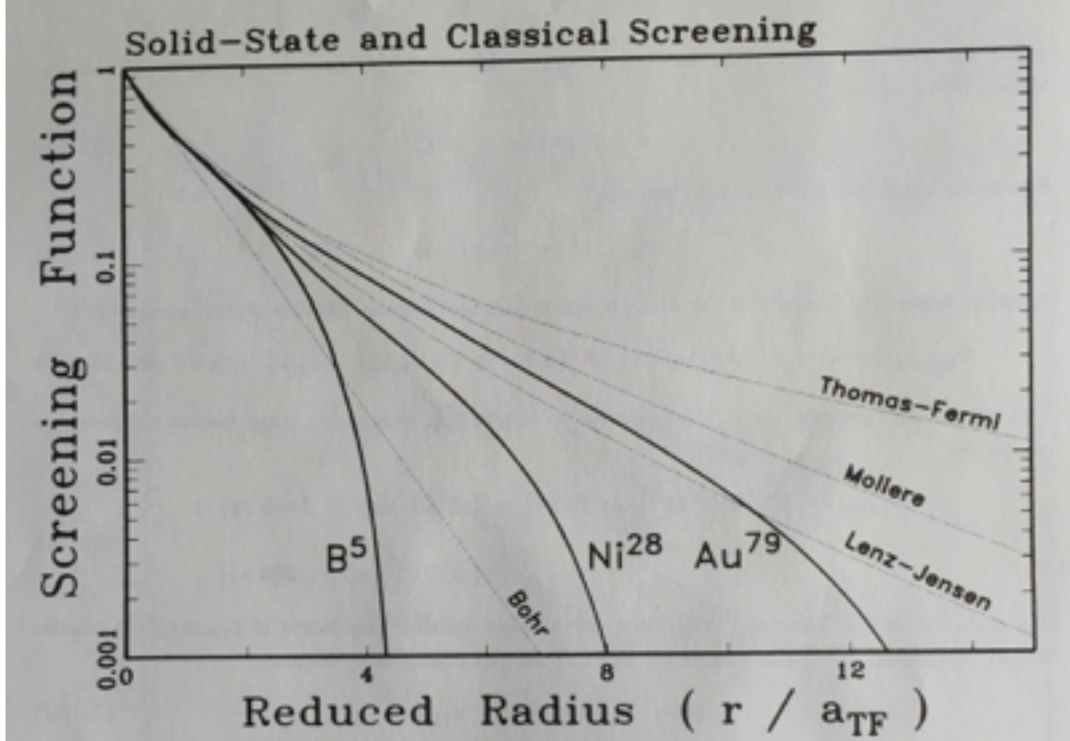

Figure (2-7) The screening function of three solid-state atomic charge distributions and four classical screening functions. The solid-state atomic charge distributions are tabulated in the Appendix. The nickel and gold atoms are from f.c.c. structures, while the boron is from a hexagonal structure. The screening functions are calculated using equation (2-44). For the inner shells, these atoms are well described by the Moliere and Lenz-Jensen atoms. Beyond the L-shell, none of the classical screening functions adequately describe the solid-state screening.

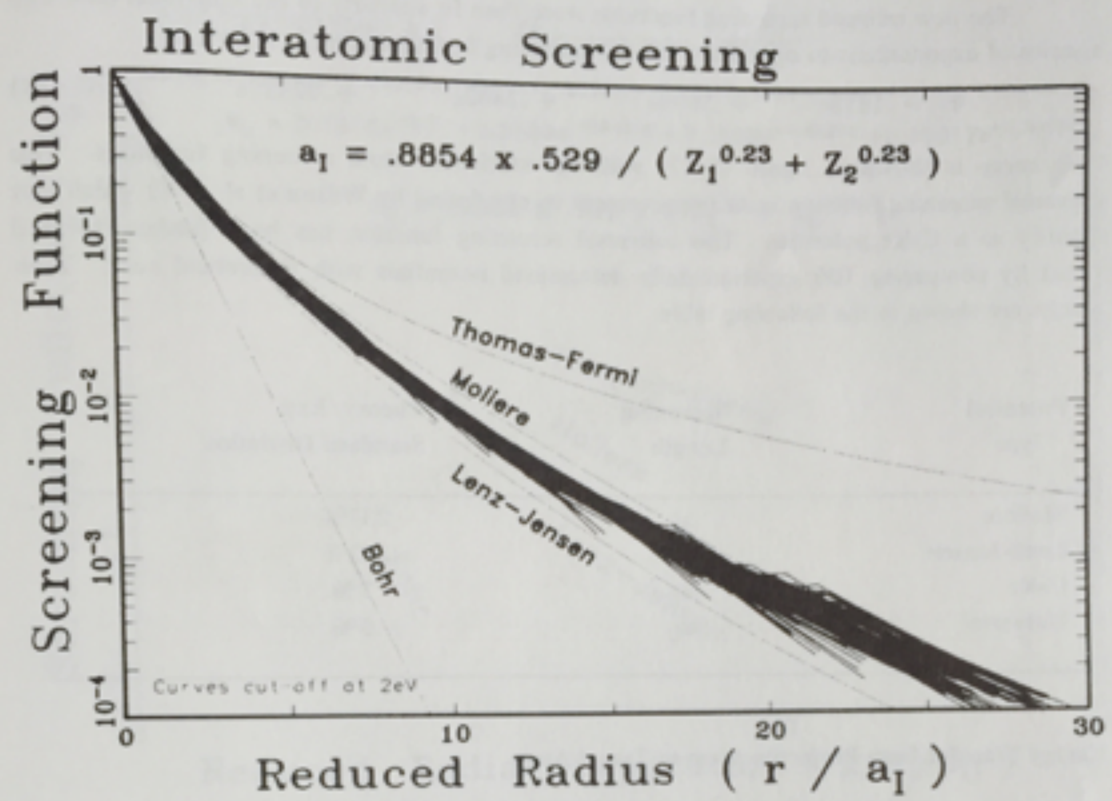

Figure (2-16) The screening functions of figure (2-14) are compacted further by introducing the new screening factor shown above, which calculates the screening length by using a factor of 0.23 for Z_1 and Z_2. The grouping is quite tight, with a standard deviation, $\sigma \approx 18\%$. With this new screening distance, a_I, all the interatomic potentials can be calculated with reasonable accuracy. Further, this screening length can now be used to generate universal nuclear stopping powers with a simple analytic expression.

Phys Rev B 24 4999 (1981)

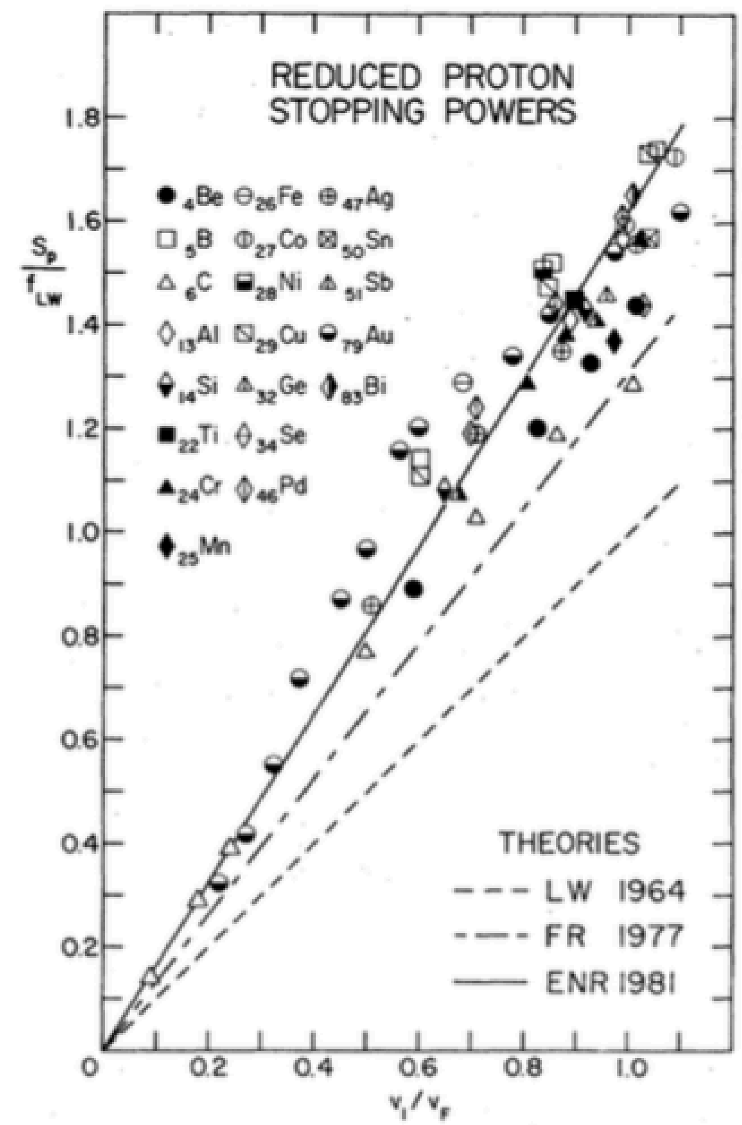

FIG. 2. Stopping powers for protons in the reduced form $S/f_{\rm LW}$ vs v_1/v_F, where $f_{\rm LW}$ is Eq. (4). Experimental data from Ref. 20. Theoretical lines depict low-velocity stopping powers, Eq. (1), in the form $S/f_{\rm LW}=(f/f_{\rm LW})(v_1/v_F)$. The constants $f/f_{\rm LW}$ are shown in Fig. 1. The broken line represents the Lindhard-Winther (LW) approximation, Eq. (4), curve III in Fig. 1, the line of dots and dashes the Ferrell-Ritchie (FR) approximation, curve V in Fig. 1, the solid line the Echenique-Nieminen-Ritchie (ENR) approximation, curve V in Fig. 1.